

INFLUENCE OF ETHYL SILICATE ON THE STRUCTURAL AND MORPHOLOGICAL PROPERTIES OF CALCIUM-PHOSPHATE SOL-GEL DERIVED GLASSES

F. TALOS^{1,*}, A. VULPOI¹, S. SIMON¹

ABSTRACT. Structural organization induced by using different concentration of ethyl silicate in the bioactive $\text{SiO}_2\text{-CaO-P}_2\text{O}_5$ sol-gel glasses, using Fourier transforms infrared spectroscopy (FTIR), X-ray powder diffraction (XRD) and Scanning Electron Microscopy (SEM) was investigated in the present study. Additionally, the incorporation of calcium oxide into glass structure during different heat treatments was also examined. After the thermal treatment at 700°C , XRD patterns evidenced the presence of new calcium phases: calcium pyrophosphate ($\text{Ca}_2\text{P}_2\text{O}_7$) and calcium silicate ($\text{Ca}_6(\text{SiO}_4)(\text{Si}_3\text{O}_{10})$). FTIR spectra also revealed that after annealing the highest CaO content produces a faster depolymerization of silica network.

Keywords: *sol-gel, FTIR, XRD, SEM, $\text{Ca}_2\text{P}_2\text{O}_7$, $\text{Ca}_6(\text{SiO}_4)(\text{Si}_3\text{O}_{10})$.*

INTRODUCTION

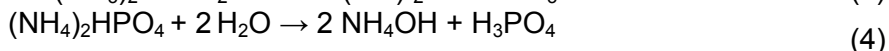
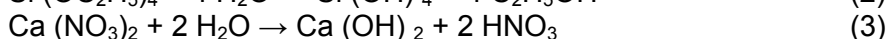
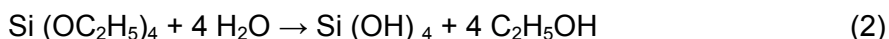
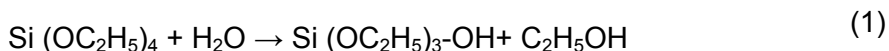
The rapid development of nanostructure materials presents scientific and technical challenges for the design and fabrication of bioactive materials at low synthesis temperature used for biomedical applications. Hench *et al.* used for the first time the term "bioactive glasses" to describe the interfacial bond of silicate-based with calcium and phosphate glasses with the physiological environments [1]. The used synthesis involved in that study provides a high temperature melt-quenching procedure but, twenty years later, the same group showed that the sol-gel process allows the synthesis of high purity, homogeneous materials. Moreover, porous structure can be controlled by modifying the precursor's concentration [2]. In particular, the gel strength of the silica matrix has been modulated, leading to the development of new materials with special properties, such as biosensors, bioreactors [3], encapsulation of bio species [4-6], bioactive glass microspheres [7], drug delivery [8] and hybrid organic-inorganic materials [9]. The tetra-ethyl silicate $\text{Si}(\text{OR})_4$, where $\text{R} = \text{C}_2\text{H}_5$, usually is mixed together with an alcoholic solution in the presence of an acid catalysis and these reactions can be described as

¹ Institute of Interdisciplinary Research in Bio-Nano-Sciences, 42 Treboniu Laurian, 400271 & Faculty of Physics, Babeş-Bolyai University, 1 Mihail Kogalniceanu, 400084, Cluj-Napoca, Romania
* florentina.talos@ubbcluj.ro

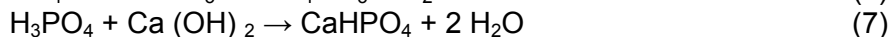
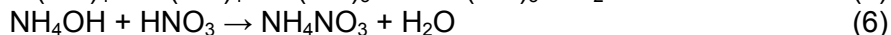
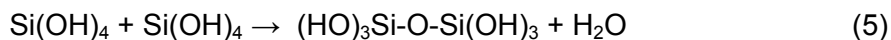
an SN_2 nucleophilic substitution. Also, in acidic condition, hydrolysis is relatively faster than condensation, and weakly branched polysiloxane network usually are formed [10]. Thus chemical gels created via sol-gel process provide strong covalent bonding where their cross-links are irreversible [11]. During the ageing stage of the sol-gel process, it was attested that the calcium nitrate is dissolved in the pores, which are generated by the products of the condensation reaction. In addition, during the drying process, calcium nitrate is deposited on the gel surface and further heat treatments provide the diffusion of calcium in the network [12]. Moreover, phosphorus and silicon are considered to be both nucleation agents as well as network formers.

The possible hydrolysis-condensation reactions of sol-gel materials in the presence of salts are presented below:

Hydrolysis



Condensation



The present study aims to synthesize homogeneous polysiloxane gels with inorganic salts at a relatively low pH starting from a non - aqueous solution. To accomplish this purpose, two different concentration of silicon alkoxide (4Si, 2Si) were used in order to obtain materials with controlled morphology, designed for further biomedical applications. Furthermore, structural and morphological modification after drying and annealing were characterized by means of XRD, FTIR, TEM and SEM techniques, respectively.

RESULTS AND DISCUSSION

The structural phases for the dried and 1 hour thermally treated materials at 700°C were characterized by XRD and are shown in Fig.1 (a-b).

The XRD patterns for the 4Si and 2Si samples after being dried at 100°C exhibit peaks corresponding to un-reacted ammonium nitrate NH_4NO_3 phase. By increasing the temperature at 700°C the 2Si and 4Si samples revealed peaks

corresponding to calcium pyrophosphate ($\text{Ca}_2\text{P}_2\text{O}_7$) and calcium silicate ($\text{Ca}_6(\text{SiO}_4)(\text{Si}_3\text{O}_{10})$) phases, overlapped on the amorphous matrix. The appearance of these phases is inhibited by the higher silicate concentration.

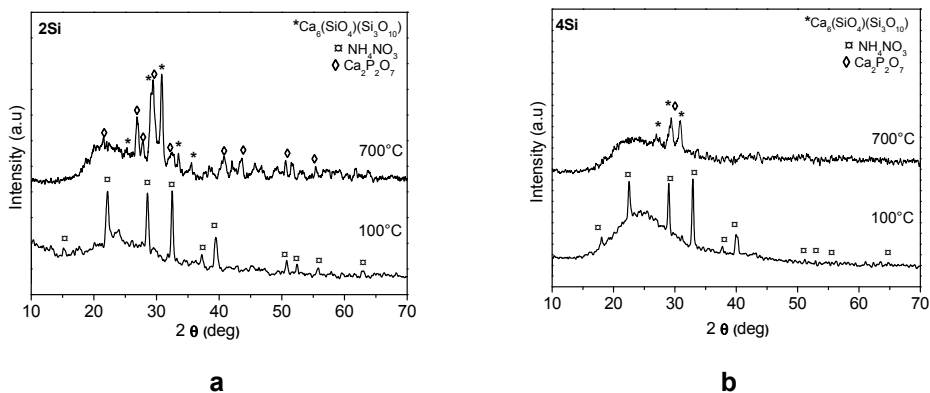


Figure 1. XRD patterns of the glass samples, dried at 100°C and after thermal treatment at 700°C: (a) 2Si; (b) 4Si.

In order to obtain more detailed information about the structural changes observed in the XRD patterns, FTIR study has been carried out for these samples. Room-temperature IR spectra of 4Si, 2Si glass samples are presented in Fig. 2.

The 2Si and 4Si dried samples (Fig. 2 (a, b)) present a series of infrared bands located at: 465, 825, 950, 1080, 1129, 1227, 1375, 1637, 2430, 3750 cm^{-1} . The broad absorption band situated between 3750 cm^{-1} and 2910 cm^{-1} becomes larger after thermal treatment. This band is assigned to bending and stretching vibration -OH of molecular water [13]. The peak at 3450 cm^{-1} is associated to silanol groups linked to molecular water through hydrogen bonds. Among 3000-2800 cm^{-1} are located the bands ascribed to the symmetric and asymmetric fundamental stretching vibration of CH_2 and CH_3 groups from the residues of the precursors used in the sol-gel synthesis. The signal recorded at around 1620 cm^{-1} is due to the deformation modes of O-H groups and absorbed water molecules, δ (H-O-H) [13]. The shoulder at 1640 cm^{-1} changes to a smaller one after heating at 700°C.

Moreover, the sharp peak assigned to the nitro group ($-\text{NO}_2$) is isoelectric with the carboxylate ion groups ($-\text{CO}_2$), both providing very similar spectra for the main functional group and both being located around 1380 cm^{-1} , observed in all dry gels (2Si and 4Si) [14]. This peak disappears in both 2Si and 4Si glasses after annealing at higher temperatures. The small shoulder situated around 1152 cm^{-1} can be ascribed to the longitudinal optical Si-O-Si stretching

vibration [13]. Furthermore, the shoulder situated around 1080 cm^{-1} is attributed to the asymmetric stretching mode of Si-O-Si (asym) bonds in the tetrahedral units, while the shoulder centred at 950 cm^{-1} is attributed to the Si-O-Ca bonds containing non-bridging oxygen [15]. Analysis has revealed also a component at 800 cm^{-1} , assigned to silicon-oxygen symmetric stretching vibration modes. The lower vibrational frequencies may be characteristic to P-O-P linkages in polymeric systems, the ones between 700 cm^{-1} and 770 cm^{-1} corresponds to pyro-phosphates $(\text{P}_2\text{O}_7)^{4-}$ [16]. Two small peaks at 525 and 630 cm^{-1} are associated to $(\text{O}-\text{P}=\text{H}-\text{O})$ bending mode of crystalline phosphate formed on the glasses [17]. Also a small absorption signal occurs at 470 cm^{-1} , which can be assigned to the rocking motion of the bridging oxygen atoms perpendicularly to the Si-O-Si plane [18].

An interesting feature observed in the IR spectrum of the 700°C heat treated samples compared with the dried samples, is the increased intensity of the bands located between 1150-950 cm^{-1} . This behaviour is more pronounced for the sample 2Si were the bands attributed to symmetric and asymmetric Si-O-Si respectively to Si-O-NBO presents higher intensity. We assume that lower concentration of ethyl silicate and higher concentration of CaO induces the depolymerisation of the silica matrix. More precisely, the above-mentioned modes have been assigned to different aggregation processes of silica based matrix such as $[\text{SiO}_4]^{4-}$ monomers and $[\text{Si}_3\text{O}_{10}]^{8-}$ trimers, hypothesis supported also by the XRD results. The obtained results reveal thus that CaO leads to depolymerization of silicate network after annealing process.

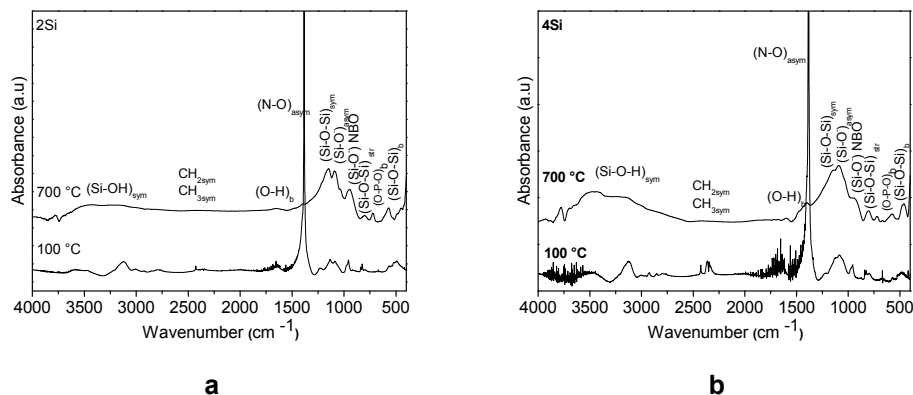


Figure 2. FTIR absorption spectra of the glass samples, dried at 100°C and after thermal treatment at 700°C: (a) 2Si; (b) 4Si.

Fig. 3 shows the SEM micrographs realized for 2Si, 4Si glasses dried at 100°C. The surface of the 2Si glasses Fig. 3. (a.I) is composed of larger spherical agglomerates with small crystals while the 4Si material (see Fig. 3. (b.I)) displays smaller particles with almost spherical morphology.

After annealing at 700 °C the surfaces of the 2Si glass (Fig. 3.a.II) reveal changes in their morphology, lamellar crystals can be seen on a surface composed by small spherical aggregates. No significant modification was observed for the 4Si samples after heating (Fig. 3.b.II). Based on XRD data (Fig. 1, and SEM images (Fig. 3), it could be concluded that new phases were formed on the materials surface; these changes are more pronounced for the 2Si sample. This outcome is due to a highest resistance at depolymerization of 4Si samples, result showed also by means of FTIR spectroscopy.

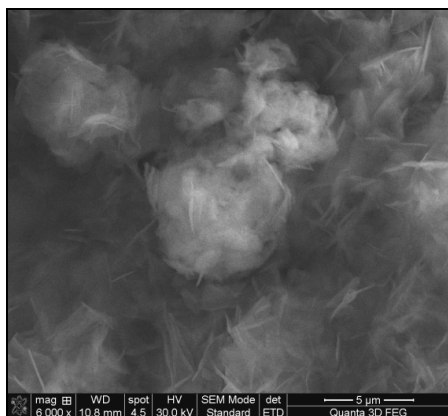
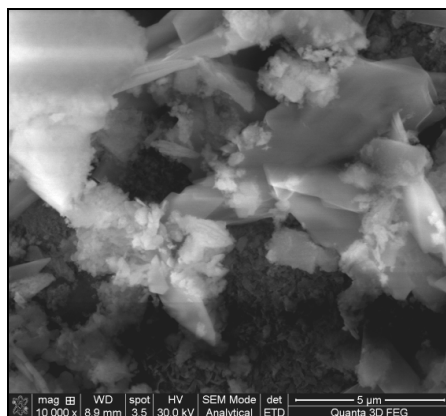
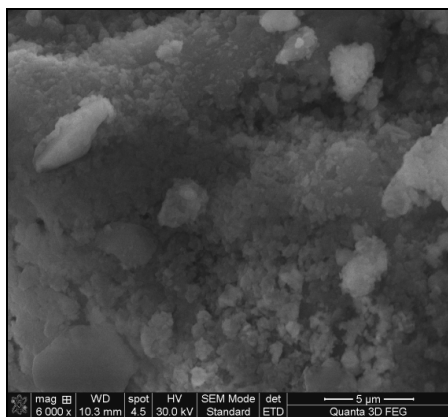
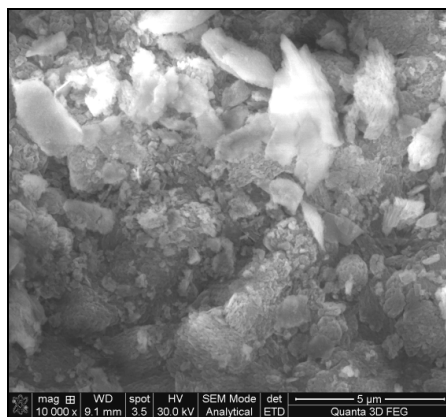
**a.I****a.II****b.I****b.II**

Figure 3. SEM micrographs of the glass samples dried at 100°C (a.I) 2Si, (b.I) 4Si and after heat treatment at 700°C (a.II) 2Si, (b.II) 4Si.

CONCLUSIONS

Homogeneous 4Si and 2Si samples have been obtained by the sol–gel method. X-ray diffraction analysis for the 4Si, 2Si system reveals crystal phases, associated with calcium pyrophosphate ($\text{Ca}_2\text{P}_2\text{O}_7$) and calcium silicate ($\text{Ca}_6(\text{SiO}_4)(\text{Si}_3\text{O}_{10})$) phases, presenting an interesting approach for the material science used in bio-applications. FTIR spectroscopy of the studied samples after their annealing at 700°C indicates the depolymerisation of the local network, resulting mainly in tetrahedral silicate units. This behaviour is more evident for the 2Si sample. The SEM micrographs achieved for the 4Si and 2Si materials prove also the morphological modification after annealing at 700°C .

EXPERIMENTAL SECTION

Two types of glasses with different compositions belonging to the $\text{SiO}_2\text{-CaO-P}_2\text{O}_5$ system have been obtained by sol–gel method (Table 1). The sol–gel precursors used in this study were tetraethyl orthosilicate (TEOS, $(\text{Si}(\text{OC}_2\text{H}_5)_4)$, calcium nitrate tetrahydrate ($\text{Ca}(\text{NO}_3)_2 \cdot 4\text{H}_2\text{O}$), di-ammonium hydrogen phosphate $(\text{NH}_4)_2\text{HPO}_4$. All the gels were prepared at room temperature (nearly 21°C).

Table.1. Nominal compositions (wt. %) of the sol–gel glasses

Glasses Name	SiO_2	CaO	P_2O_5
4Si	70,90	16,54	12,56
2Si	54,91	25,63	19,46

The sol-gel synthesis: The TEOS has been mixed with the solvent (ethanol) and stirred for 30 minutes, in 1:2 molar ratios. The calcium and phosphate salts have been separately dissolved in deionized water, according to the molar ratio 1:2, for 30 minutes. The resulted calcium and phosphorous solutions were firstly mixed together, while the pH was adjusted to 1 using nitric acid (conc. 65%) and then put over the silica solution. The final solution was stirred for 1 hour and introduced in a polyethylene cylindrical recipient at 37°C during 48 hours for aging. After drying at 100°C for 24 hours, the glass has been annealed at 700°C for 1 hour and then cooled at room temperature.

The structural changes of the dried and heat treated powders were investigated by X-ray diffraction using a Shimadzu XRD-6000 diffractometer with a monochromator of graphite for $\text{CuK}\alpha$ ($\lambda=1.54 \text{ \AA}$). The diffractograms were performed in a 2θ degree range of $10^\circ\text{--}70^\circ$ with a speed of $2^\circ/\text{min}$.

For the FTIR measurements, identical amounts of glass powder were mixed with KBr in order to obtain pellets of about 1 mm thickness. The spectra were recorded at room temperature in a 400-4000 cm^{-1} spectral range with a JASCO FT/IR-6200 infrared spectrometer using a maximum resolution of 4 cm^{-1} and 256 scans. Each spectrum was scanned for 32 times to increase the signal-to-noise ratio. The FTIR spectra were performed for the dried and 700°C heat treated samples.

The morphology and microstructure of the prepared composite samples were investigated by scanning electron microscopy (SEM). The SEM images were recorded using FEI QUANTA 3D FEG dual beam, which work in high vacuum mode. In order to amplify the secondary electrons signal a cover of 5 nm thickness was performed with Pt-Pd into Agar Automatic Sputter Coater, in Ar atmosphere.

ACKNOWLEDGMENTS

This research was accomplished in the framework PNII IDEI - PCCE 101/2008 PROJECT from the Romanian National University Research Council - CNCSIS. F. Taloş author wishes to thank for the financial support provided from programs co-financed by the Sectoral Operational Programme Human Resources Development POSDRU/88/1.5/S/60185-INNOVATIVE DOCTORAL STUDIES IN A KNOWLEDGE BASED SOCIETY.

REFERENCES

1. L.L. Hench, R.J. Splinter, W.C. Allen, T.K. Greenlee, *Journal of Biomedical Materials Research Part A2*, **1971**, 2, 117.
2. M.M. Pereira, A.E. Clark and L.L. Hench, *Journal of Biomedical Materials Research Part A2*, **1994**, 28, 693.
3. M.L. Ferrer, D. Levy, B. Gomez-Lor, M. Iglesias, *Journal of Molecular Catalysis B - Enzymatic*, **2004**, 27, 107.
4. J.Y. Barreau, J.M. DaCosta, I. Desportes, J. Livage, L. Monjour, M. Gentilini, *Comptes rendus de l'Academie des sciences, Serie III Sciences de la vie*, **1994**, 317, 653.
5. J. Livage, C. Roux, J.M. Costa, I. Desportes, J.F. Quinson, *Journal of Sol-Gel Science and Technology*, **1996**, 7, 45.
6. C. Roux, J. Livage, K. Farhati and L. Monjour, *Journal of Sol-Gel Science and Technology*, **1997**, 8, 663.

7. D. Caccina, R. Viitala, M. Jokinen, H. Ylänen, M. Hupa, S. Simon, *Key Engineering Materials*, **2005**, 284-286, 411.
8. M. Goldenberg, R. Langer, X. Jia, *Journal of Biomaterials Science, Polymer Edition*, **2007**, 18, 241.
9. C. Sanchez, B. Julian, P. Belleville and M. Popall, *Journal of Materials Chemistry*, **2005**, 15, 3559.
10. C.J. Brinker and G.W. Scherer, "The Physics and Chemistry of Sol-Gel Processing", Academic Press, Inc., San Diego, **1990**.
11. T. Miura, H. Okumoto, H. Ichijo, *Physical Review E*, **1996**, 54, 6596.
12. S. Lin, C. Ionescu, K.J. Pike, M.E. Smith, J.R. Jones, *Journal of Materials Chemistry*, **2009**, 19, 1276.
13. G. Socrates, "Infrared and Raman Characteristic Group Frequencies, Tables and Charts", John Wiley and Sons, Ltd., Chichester, UK, **2001**.
14. John Coates, "Interpretation of Infrared Spectra, A Practical Approach. Encyclopedia of Analytical Chemistry", R.A. Meyers, John Wiley & Sons Ltd, Chichester, **2000**, chapter 3.
15. P. Saravanapavan, L.L. Hench, *Journal of Non-Crystalline Solids*, **2003**, 318, 1.
16. A. Gozalian, A. Behnamghader, M. Daliri, A. Moshkforoush, *Scientia Iranica F*, **2011**, 18, 1614.
17. S. Shahrabi, S. Hesarak, S. Moemeni, M. Khorami, *Ceramics International*, **2011**, 37, 2737.
18. A. Chrissanthopoulos, N. Bouropoulos, S.N. Yannopoulos, *Vibrational Spectroscopy*, **2008**, 48, 118.